

GENERALIZED COMPLEX 2D MATCHED FILTERING FOR LOCAL REGULAR LINE-LIKE FEATURE DETECTION

Mihails Pudzs, Modris Greitans, and Rihards Fuksis

Institute of Electronics and Computer Science
14 Dzerbenes Str., Riga, LV1006, Latvia
phone: + (371) 67558238, fax: + (371) 67555337
email: {Mihails.Pudzs, Modris.Greitans, Rihards.Fuksis}@edi.lv
web: http://www.edi.lv

ABSTRACT

In pattern recognition systems it is usually necessary to detect different image details, like edges, lines, corners, blobs, etc. For this purpose a bank of special filters, matching each individual detail can be used. As the details usually are oriented in different directions and have different scales, the image processing leads to many convolution operations. The *complex 2D matched filter* (CMF) is an angle invariant line detection filter, which also provides additional information about orientation of detected lines.

In this paper we follow the idea of complex matched filtering, and develop *generalized complex matched filtering* (GCMF) approach, which is a whole bank of different angle invariant filters, where each filter is denoted by the order. These filters can be used to detect a broader range of image details: edges, lines, line intersections and corners; and, like its predecessor, the GCMF provides additional information about the detected features – the orientation angle. Each kernel from the GCMF bank is analyzed in polar coordinates and the specifics of detail detection are explained. A method of generating GCMF normalized kernels of arbitrary order is proposed. GCMF algorithm is presented and its performance is demonstrated on test images.

1. INTRODUCTION

Fast feature extraction is still a significant problem in most image processing systems [3, 2]. After the image is obtained it is important to detect the desired objects and save them for further analysis. Usually the details are extracted using the convolution with a mask that is similar to the desired object. This approach is called *matched filtering* (MF) [1]. While being very effective at extracting an object from noise, it can be very slow for 2D signals, because of the need to rotate the filter kernel.

In our previous work [4] we have introduced an angle invariant method, called *complex 2D matched filtering* (CMF) which is based on the MF approach. In addition to ability to detect lines in images, CMF also obtains their angular orientation. CMF uses only one complex kernel instead of many rotated masks, therefore, it is more computationally efficient than the MF approach.

This paper is devoted to the further development of the CMF idea and the analysis of its specific properties. As a result, the *generalized complex matched filtering* (GCMF) approach is presented. For each used order GCMF requires one convolution operation with the complex kernel, therefore, it can be used in embedded systems when different lines and their crossings have to be detected.

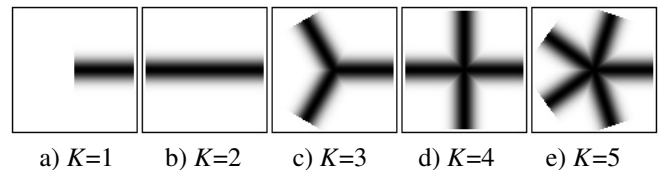


Figure 1: MF masks (M_K) of first 5 orders, used by CMF $_K$

2. COMPLEX MATCHED FILTERING

For consistency with the GCMF notation, equations that are given here, will contain the index "2", because CMF is the second order filter from the GCMF bank. As mentioned before, the CMF is based on the MF approach, and in its full form requires MF of the image with a line-detecting mask (see Fig.1b) of all non-recurring directions $\varphi_{2,n} \in [0; \pi)$, where n is the index number. As a result, the set of MF scalar responses of $s_{2,n}(\varphi_{2,n}; x, y)$ are obtained in each pixel. The main idea of CMF is the principle of combining these responses into a single complex value (*matching intensity vector* [4]) that describes the filtered object.

For this purpose:

1. The scalar responses are transformed into the complex ones by assigning the phase value of $2\varphi_{2,n}$.

$$\vec{c}_{2,n}(\varphi_{2,n}) = s_{2,n}(\varphi_{2,n}) \exp(j2\varphi_{2,n}); \quad (1)$$

2. The complex responses are summed together:

$$\vec{c}_2 = \sum_{n=0}^{N-1} \vec{c}_{2,n}(\varphi_{2,n}); \quad (2)$$

3. Finally, matching intensity vector is acquired from the sum by decreasing its angle by half.

The short form of CMF utilizes the property of superposition, and reduces the operations count by combining multiple MF masks $M_2(x, y; \varphi_{2,n})$ into one complex mask $\underline{M}_2(x, y)$.

$$\underline{M}_2(x, y) = \sum_{n=0}^{N-1} e^{j2\varphi_{2,n}} M_2(x, y; \varphi_{2,n}) \quad (3)$$

In the next sections all mentioned steps are discussed thoroughly, using equations in general form.

3. GENERALIZATION OF CMF

Further, K will denote the order of complex matched filter (CMF $_K$), matched filter mask (M_K), or the complex mask

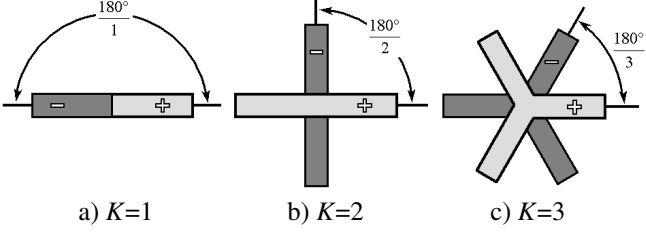


Figure 2: Rotated MF masks with opposite behavior

(\underline{M}_K). The extended approach needs a specific set of MF masks to be generated. We begin building (M_K) masks with one line that connects the center of the mask with its edge (Fig. 1a). This is the first order MF mask, or (M_1). Then we add more lines (one by one), and each time distribute all lines regularly to form even angles between them. Each added line increases the order of the MF mask (M_K). The Fig. 1 shows the first 5 orders of MF masks ($M_1 - M_5$) that will be used by the CMF of the orders $\text{CMF}_1 - \text{CMF}_5$.

Each MF mask $M_K(\varphi_{K,n})$ is rotated around its center in the angular interval of $\varphi_{K,n} \in [0; \frac{2\pi}{K})$ to avoid filtration with the identical kernel more than once:

$$\varphi_{K,n} = \frac{n \cdot 2\pi}{N \cdot K} \quad (4)$$

where $n = 0 \dots (N-1)$, N - total number of MF mask angles used (specifies the angular precision). The MF response at the particular point (x_0, y_0) can be formally expressed as:

$$s_{K,n}(x_0, y_0; \varphi_{K,n}) = \iint_D f(x, y) M_K(x - x_0, y - y_0; \varphi_{K,n}) dx dy \quad (5)$$

where $f(x, y)$ is the image being filtered, and D - the MF mask's M_K overlay area.

After MF at different angles, the scalar MF responses obtained $s_{K,n}(\varphi_{K,n})$ are transformed into complex responses $\vec{c}_{K,n}(\varphi_{K,n})$ by assigning the phase value.

The generalized approach assigns opposite phases to the MF responses from masks that have *opposite behavior*, which, in general, is characteristic for pairs of MF masks of the same order with an angular difference of $\Delta\varphi_K = \frac{180^\circ}{K}$. Figure 2 shows three examples of rotated MF masks with opposite behavior. It is obvious that when the angle of $K \cdot \varphi_{K,n}$ is assigned to the matched filter reactions, all MF reaction pairs behaving contrarily, are transformed into antiphase complex reactions $\vec{c}_{K,n}$, because $K \cdot \Delta\varphi_K = K \cdot \frac{180^\circ}{K} = 180^\circ$:

$$\vec{c}_{K,n}(\varphi_{K,n}) = s_{K,n}(\varphi_{K,n}) \exp(jK\varphi_{K,n}) \quad (6)$$

The GCMF result is obtained by summing all the complex reactions together:

$$\vec{c}_K = \sum_{n=0}^{N-1} \vec{c}_{K,n}(\varphi_{K,n}) \quad (7)$$

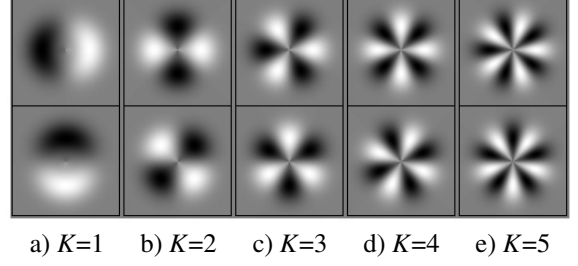


Figure 3: First five GCMF kernels generated using Eq. (16) and (17): the top row is the real part, the bottom row - the imaginary part

Using generalized equation (6), (7) is rewritten as:

$$\begin{aligned} \vec{c}_K(x_0, y_0) = & \sum_{n=0}^{N-1} e^{jK\varphi_{K,n}} \iint_D f(x, y) M_K(x - x_0, y - y_0; \varphi_{K,n}) dx dy = \\ & \iint_D f(x, y) \left[\sum_{n=0}^{N-1} e^{jK\varphi_{K,n}} M_K(x - x_0, y - y_0; \varphi_{K,n}) \right] dx dy \end{aligned} \quad (8)$$

It leads to the conclusion that the complex sum $\vec{c}_K(x, y)$ can be obtained using one convolution operation with the complex kernel:

$$\underline{M}_K(x, y) = \sum_{n=0}^{N-1} e^{jK\varphi_{K,n}} M_K(x, y; \varphi_{K,n}) \quad (9)$$

The last expression defines the GCMF mask of order K , and extends the previous concept of complex 2D matched filtering.

4. GCMF KERNEL ANALYSIS

For maximum angular precision, φ is used instead of $\varphi_{K,n}$, and summation in eq. (9) is replaced with the integration by $d\varphi$:

$$\underline{M}_K(x, y) = \int_0^{\frac{2\pi}{K}} e^{jK\varphi} M_K(x, y; \varphi) d\varphi \quad (10)$$

The analysis of GCMF kernel \underline{M}_K is done in polar coordinates (ρ, θ) , by analyzing the eq. (10). For convenience, let the filter kernels be located at $(0, 0)$, and the point of interest to be (ρ, θ) . The GCMF kernel value $\underline{M}_K(\rho, \theta)$ is obtained using the rotated MF mask $M_K(x, y; \varphi)$ points $M_K(\rho, \theta - \varphi)$ that are mapped at (ρ, θ) :

$$\underline{M}_K(\rho, \theta) = \int_0^{\frac{2\pi}{K}} e^{jK\varphi} \cdot M_K(\rho, \theta - \varphi) d\varphi \quad (11)$$

Values of the particular points of the MF mask can be obtained using the Dirac Delta function as:

$$M_K(\rho, \theta - \varphi) = \int_0^{2\pi} M_K(\rho, \tau) \cdot \delta(\rho, \tau - [\theta - \varphi]) d\tau \quad (12)$$

where τ is the angular variable for MF mask "scanning". Combining (11) with (12), leads to:

$$M_K(\rho, \theta) = \int_0^{2\pi/K} \left[e^{jK\varphi} \int_0^{2\pi} M_K(\rho, \tau) \delta(\rho, \tau - [\theta - \varphi]) d\tau \right] d\varphi \quad (13)$$

which is solved by rearranging its elements as:

$$\underline{M}_K(\rho, \theta) = e^{jK\theta} \cdot \int_0^{2\pi} M_K(\rho, \tau) e^{-jK\tau} d\tau \quad (14)$$

Equation (14) defines the GCMF kernel. This equation eliminates the need to rotate MF masks, like it was done previously in (9).

The right part of (14) consists of two multipliers:

- $e^{jK\theta}$ is the *angular component of the complex mask*. This component is order dependent.
- $\underline{r}(\rho) = \int_0^{2\pi} M_K(\rho, \tau) \cdot e^{-jK\tau} \cdot d\tau$ is called as *radial component of the complex mask*. This component varies only with distance from the center of the complex mask and defines the magnitude of the angular component.

The scalar product of two complex masks demonstrates the orthogonality of GCMF kernels and leads to the conclusion that each CMF_K extracts unique information $\vec{c}_K(x, y)$ from the filtered image.

$$\begin{aligned} (\underline{M}_K; \underline{M}_L^*) &= (e^{jK\theta} \underline{r}(\rho); e^{-jL\theta} \underline{r}^*(\rho)) \\ &= \delta_{K,L} 2\pi \int_0^P r^2(\rho) \rho d\rho \end{aligned} \quad (15)$$

where $\delta_{K,L}$ is the Kronecker's delta, $r(\rho) = Re[\underline{r}(\rho)]$, P is complex mask radius, and $*$ denotes the complex conjugate. The (15) with $K = L$ describes the squared norm of GCMF kernel (14). By normalizing (14), the equation for efficient generation of orthonormal GCMF kernels is obtained:

$$\underline{M}_K(\rho, \theta) = \frac{e^{jK\theta} r(\rho)}{\sqrt{2\pi \int_0^P r^2(\rho) \rho d\rho}} \quad (16)$$

The radial component $r(\rho)$ is chosen depending on the scale of features to extract, and, to preserve orthonormality, it must be the same for the whole set of GCMF kernels if many different orders are used together. For example, the following radial component might be used:

$$r(\rho) = \exp\left[-\frac{(\rho - 1.5\sigma)^2}{\sigma^2}\right] + \exp\left[-\frac{(\rho + 1.5\sigma)^2}{\sigma^2}\right] \quad (17)$$

Then, the GCMF would detect details with a diameter of approximately 5σ , but P should be at least 3.5σ . Figure 3b is similar to the complex mask, proposed in [4].

Filters with kernels that are similar to GCMF have been introduced previously. For example, *Gaussian derivative*

kernels in [7] are generated as the linear combination of the Cartesian derivatives of Gaussian function L . For example, $L_x = \frac{\partial L}{\partial x}$ and $L_y = \frac{\partial L}{\partial y}$ are similar to CMF_1 complex kernel's real and imaginary parts (Fig.3a); $L_{xy} = \frac{\partial^2 L}{\partial x \partial y}$ is similar to CMF_2 complex kernel's imaginary part (Fig. 3b). Despite of this similarity, we, however, provide different bank of kernels, and analyze them in polar coordinate system, not in Cartesian. Another similar approach can be found in [6, 8, 9]. These filters are called *radial spiculation filters* (RSF), and are of two types: Sine RSF, and Cosine RSF. The CRSF and SRSF are defined by equations:

$$CRSF = e^{-\frac{(\rho-\rho_0)^2}{2\sigma^2}} \cdot \cos(K \cdot \theta) \quad (18a)$$

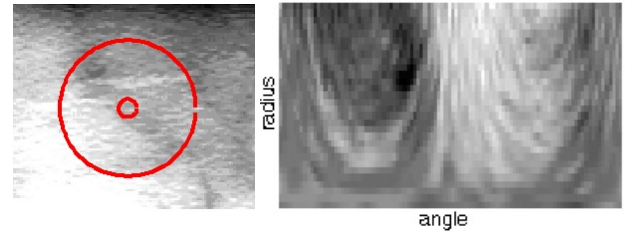
$$SRSF = e^{-\frac{(\rho-\rho_0)^2}{2\sigma^2}} \cdot \sin(K \cdot \theta) \quad (18b)$$

After applying the Euler's formula to (18), we acquire:

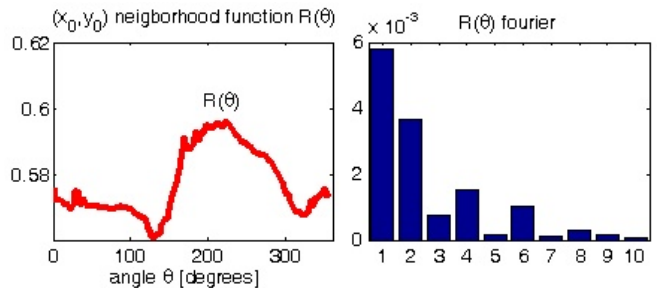
$$CRSF + j \cdot SRSF = e^{-\frac{(\rho-\rho_0)^2}{2\sigma^2}} \cdot e^{jK\theta} \quad (19)$$

Note that (19) is a particular case of GCMF kernel (13), where $e^{-\frac{(\rho-\rho_0)^2}{2\sigma^2}}$ is the radial component $r(\rho)$. Therefore, all analysis from the next sections of this paper is also applicable to RSF.

The difference between our approach and RSF is that after filtering they analyze only the magnitude of the result to get the information about density of spiculated masses. We also analyze the phase of calculated matching intensity vectors to obtain additional information about extracted features (angular orientation).

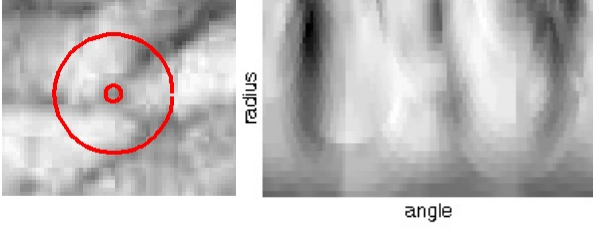


(a) Line in Cartesian (left) and polar (right)

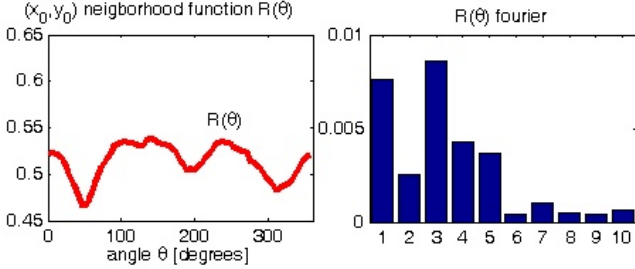


(b) Neighborhood function and its Fourier series

Figure 4: Example of line detection with CMF_2



(a) Line intersection in Cartesian (left) and polar (right)



(b) Neighborhood function and its Fourier series

Figure 5: Line intersection detection with CMF_3

5. GCMF NEIGHBORHOOD FUNCTION

Using GCMF Eq. (14) we can rewrite the Eq. (8) to formally describe the complex matched filtering process as:

$$\vec{c}_K(x_0, y_0) = \iint_D f(x, y) \underline{M}_K(x - x_0, y - y_0) dx dy \quad (20)$$

The complex mask $\underline{M}_K = e^{jK \cdot \theta} \cdot \underline{r}(\rho)$ is located at the point of interest (x_0, y_0) and is described using polar coordinates (ρ, θ) that are mapped onto (x, y) with center in the (x_0, y_0) . Further, only these mapped polar coordinates are used:

$$\begin{aligned} \vec{c}_K(x_0, y_0) &= \iint_D f(\rho, \theta) e^{jK \cdot \theta} \underline{r}(\rho) \rho d\rho d\theta \\ &= \int_0^{2\pi} \left[\int_0^P f(\rho, \theta) \cdot \underline{r}(\rho) \rho d\rho \right] e^{jK \cdot \theta} d\theta \end{aligned} \quad (21)$$

The value in square brackets is further denoted as the pixel's (x_0, y_0) neighborhood function:

$$\underline{R}(\theta) = \int_0^P f(\rho, \theta) \cdot \underline{r}(\rho) \rho d\rho \quad (22)$$

CMF_K calculates K -th coefficient of the neighborhood function's complex Fourier series:

$$\vec{c}_K(x_0, y_0) = \left[\int_0^{2\pi} \underline{R}(\theta)^* \cdot e^{-jK \cdot \theta} d\theta \right]^* \quad (23)$$

Fig.4 and Fig.5 demonstrate how different image details appear as neighborhood function harmonics, which can be detected by (23). For example, note the gradient in Figure 4 appearing as the first harmonic and the line, appearing as the second harmonic of $\underline{R}(\theta)$; or how the third harmonic of $\underline{R}(\theta)$ indicates the vessels intersection point in Figure 5.

6. MATCHING INTENSITY VECTORS

After CMF_K , the orientation of the detected feature is obtained by solving the proportion between the phase θ of the corresponding $\underline{R}(\theta)$ harmonic and the detail's orientation angle ψ as: $\psi = \theta/K$.

Therefore, the following algorithm of GCMF is proposed:

1. $\vec{c}_K = c_K \cdot e^{j\theta} = CMF_K[f(x, y)]$,
2. $\vec{v}_K = v_K \cdot e^{j\psi} = c_K \cdot e^{j\frac{\theta}{K}}$.

Vectors \vec{v}_K are called *matching intensity vectors* and show the intensity of the mask's correlation with the image fragment as well as the orientation of the detected feature. The CMF_1 is similar to the first two steps of the Canny Edge detection algorithm, that include gradient calculation of the smoothed input image [3]. The first order matching intensity vectors \vec{v}_1 show the direction, and the rate of change of image pixels intensity, and are normal to the object edges.

The CMF_2 is used to detect blood vessels in [5]. The second order matching intensity vectors \vec{v}_2 point in the direction of detected lines.

Other GCMF can be used to detect line crossings. In cases of $K \geq 3$, the obtained phase $\psi = Arg[\vec{v}_K(x_0, y_0)]$ describes the direction of only one of the intersecting lines (the one in the angular interval of $[0; \frac{2\pi}{K})$). The direction of the others can be obtained as $\psi \pm k \cdot \frac{2\pi}{K}$, where $k = 1, 2, 3, \dots$. Figure 6 demonstrates the relation between the phase of matching intensity vector, and the directions of intersecting lines, for case of $K = 3$.

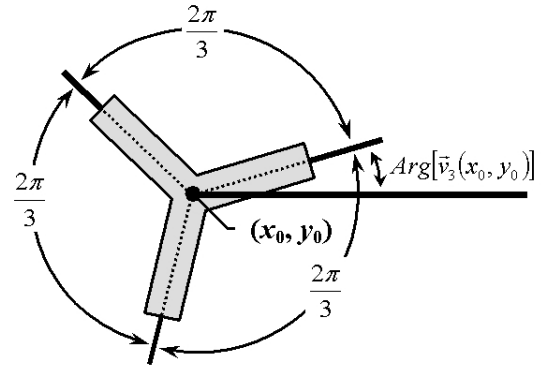


Figure 6: Matching intensity vector phase

For demonstration purposes this was done in Fig. 7 c) and d), which shows the mesh vertexes, detected by CMF_4 . Alternatively, Fig. 7 a) and b) demonstrate blood vessel detection by CMF_2 . In each case we obtain additional information of the detail orientation, performing only one convolution operation with the complex mask. The Halo artifact, mentioned in our earlier work [5] is also present in the higher order ($K > 2$) CMF_K , further research is therefore necessary on its removal. Matching intensity vectors that represent the Halo artifact are oriented differently from vectors of the desired objects, and, for demonstration purposes, in Fig. 7 b) and d) colored in gray.

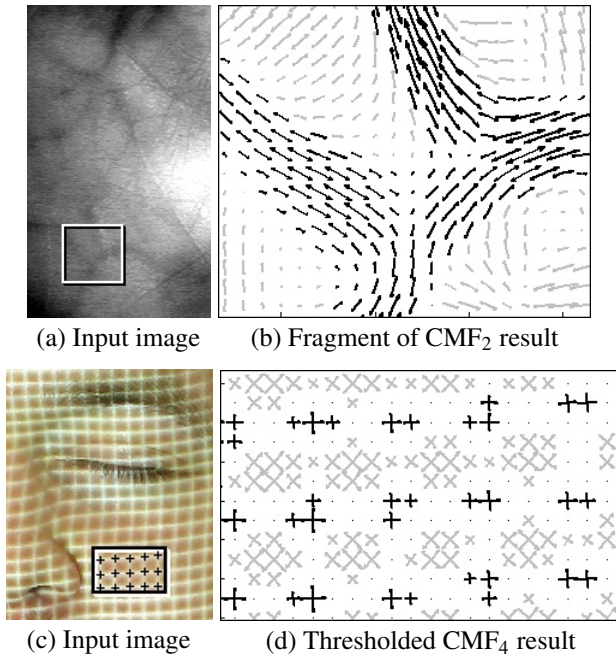


Figure 7: Examples of CMF_2 and CMF_4

7. CONCLUSIONS

We have described a generalized complex 2D matched filtering approach for the regular line-like feature, that include edges, lines, line crossings and corners, extraction from images. A mathematical form for filter kernel generation and it's relationship with matched filtering is explained. Using only one convolution operation with the complex mask, GCMF is able to detect corresponding details of different orientations, and also scales, if an appropriate radial component is chosen.

In section 5, the dual interpretation of GCMF has been shown: image convolution with complex mask is equivalent to the calculation of each pixel's neighborhood function's complex Fourier series coefficients.

Among the previously known filtering approaches, the most attractive property of GCMF approach is the ability to execute one convolution with the generated complex mask, extract the line-like objects and obtain their angular information, therefore simplifying the segmentation task.

Higher order filters ($K > 1$) produce the unwanted Halo artifact around the detected objects, so further research is necessary on how to remove it, or use it in our advantage.

Also, studies could be carried out into how different radial components or different orthogonal bases for angular component of the complex mask affect the filter properties and performance.

CMF_2 was successfully used for the extraction of palm blood vessels from images in biometric system in [5].

REFERENCES

- [1] S. Chaudhuri, S. Chatterjee, N. Katz, M. Nelson, and M. Goldbaum. Detection of blood vessels in retinal images using two-dimensional matched filters. In *IEEE Transactions on Medical Imaging, Vol.8, Issue:3*, pages 263–269. IEEE, 1989.
- [2] E. Davies. *Machine vision: theory, algorithms, practicalities*. Morgan Kaufmann, third edition, 2005.
- [3] R. C. Gonzalez and R. E. Woods. *Digital image processing*. Prentice Hall, third edition, 2007.
- [4] M. Greitans, M. Pudzs, and R. Fuksis. Object analysis in images using complex 2d matched filters. In *EUROCON 2009: Proceedings of IEEE Region 8 conference*, pages 1392–1397. IEEE, 2009.
- [5] M. Greitans, M. Pudzs, and R. Fuksis. Palm vein biometrics based on infrared imaging and complex matched filtering. In *MM&Sec '10: Proceedings of the 12th ACM workshop on Multimedia and security*, pages 101–106, New York, NY, USA, 2010. ACM.
- [6] R. Jahanbin, M. Sampat, G. Muralidhar, G. Whitman, A. Bovik, and M. Markey. Automated region of interest detection of spiculated masses on digital mammograms. In *Image Analysis and Interpretation, 2008. SSIAI 2008. IEEE Southwest Symposium on*, pages 129 – 132, 2008.
- [7] T. Lindeberg. Principles for automatic scale selection. Technical report isrn kth/na/p-98/14-se, Computational Vision and Active Perception Laboratory (CVAP), Department of Numerical Analysis and Computing Science, KTH (Royal Institute of Technology), 1998.
- [8] M. Sampat and A. Bovik. Detection of spiculated lesions in mammograms. In *Engineering in Medicine and Biology Society, 2003. Proceedings of the 25th Annual International Conference of the IEEE*, volume 1, pages 810 – 813, 2003.
- [9] M. Sampat, A. Bovik, M. Markey, G. Whitman, and T. Stephens. Toroidal gaussian filters for detection and extraction of properties of spiculated masses. In *Acoustics, Speech and Signal Processing, 2006. ICASSP 2006 Proceedings.*, volume 2, pages 593 – 596, May 2006.